

Design of a Highly Biomimetic and Fully-Actuated Robotic Finger

Li Tian, Nadia Magnenat Thalmann and jianmin
Zheng
NANYANG Technological University
Singapore 637553
tianli@ntu.edu.sg

Daniel Thalmann
EPFL IC-DO
Station 14
CH-1015 Lausanne, Switzerland

Abstract—During design a mechanical structure such as a robotic finger, modeling parts and designing joints are two time-consuming steps. This paper presents a method for design and fabrication of a humanoid robotic finger that intends to mimic the human finger in terms of tendon, bones, ligaments and the pulley systems which aims to generate a mechanism rapidly. The method is inspired by the anatomy and biomechanics of human hand, and focuses on bones, joints and actuation systems, with the aim of creating a customised finger that has the similar degrees of freedom and ranges of motion of a human finger. Specifically, we propose to create the personalised 3D models of finger’s bones by adapting a template to the data acquired by scanning the real hand, which are then fabricated by 3D printing. Low cost and easy-to-get materials such as Nylon cables and silicon rubber are used to build the tendon sheaths and the joints. We design a “3 layer cascade cable driven system” built upon eight driven cables and four servo motors for simulating all possible four Degree of Freedom (DOF) of the finger. As a result, we present a highly biomimetic and fully-actuated robotic finger, which can achieve more DOFs and larger ranges of motion compared to existing humanoid robotic hands. Particularly, the experiments validate that our robotic finger is capable of achieving all 11 standard finger gestures as a human finger.

Keywords— *Biologically-inspired robots; Dexterous manipulation; Additive manufacturing*

I. INTRODUCTION

The human hand plays an important role in our daily life. It not only helps interact with objects but also helps in the communications by hand gestures. Since the first dexterous robotic hand named “Stanford/JPL hand” was created in 1983 [1], researchers and engineers never stop pursuing a copy of real human hand through particular design. However, when we compare these robotic hands’ mechanical structure to real hand’s anatomy, we still see an impassable chasm. The human hand has a very complex internal structure that makes it difficult to be simulated. Human hand consist of 27 pieces of

bones [2]. Five bones are in the palm, five fingers have totally 14 bones, and the remaining eight bones are inside the wrist. The hand also has 15 movable joints. Each finger has three joints. A naturally evolutionary complex system controls the motion of the fingers. In this system, muscles inside the fingers actuate the bones through the tendons that are linked to the bones. Ligament, synovial cavity and bursa form the finger joints and regulate the motion speed and motion range of the fingers passively. The soft skin and tissues cover the system.

Meanwhile, the human hand is a good sample for researchers to imitate in designing humanoid robotic hands. Biologically- inspired by human hand, many anthropomorphic robotic hands have been created in recent years [3]. The Shadow hand has a large actuation system that includes up to 40 actuators. These actuators give 18 degrees of freedom (DOFs) from the hand and two more DOFs from the wrist, which are close to the DOFs of a real hand (21 DOFs) [4]. Xu et al. designed and prototyped a highly biomimetic anthropomorphic robotic hand that mimics the important biomechanics of the human hand with artificial joints and ligaments including the extensor hood mechanism and the crochet joint [5]. In [6], “HR-Hand” using intrinsic and extrinsic muscles for McKibben actuators was presented, which focuses on design and fabrication of the index finger of an Anthropomorphic Prosthetic Hands (APH).

The Shadow hand uses standard shapes to compose the fingers, which lead to a traditional appearance robotic hand. Xu’s hand and “HR-Hand” is short of DOFs which cannot fully mimic the human finger’s motion range. Recently, many soft body robotics were designed, including soft body robotic hands [7]. However, most of the soft body robotic hands do not have rigid bones inside to move like a real hand [7]. Actually, so far, there is no existing human-like robotic hand that is able to simulate all 21 DOFs motions. To fabricate a humanoid robotic hand that can achieve the motions of a real human hand, we believe that one solution is to simulate all DOFs of the human hand with an anthropomorphic robotic hand. As the first step, we present a method for designing and fabricating robotic fingers. We take the middle finger as an example (Figure 1). After studying the anatomy and biomechanism of human hands, we propose to use a simple and highly biomimetic design method to realise the important motion functions of the hand.

This research is supported by the BeingTogether Centre, a collaboration between Nanyang Technological University (NTU) Singapore and University of North Carolina (UNC) at Chapel Hill. The BeingTogether Centre is supported by the National Research Foundation, Prime Minister’s Office, Singapore under its International Research Centres in Singapore Funding Initiative.



Fig. 1. Our robotic middle finger.

Our design aims to replicate dynamic characters of the human finger in terms of the DOFs, the ranges of motion (ROM) and the movement speed. The method focuses on bones, joints and actuation systems, which play an essential role in the dynamics of fingers. The main contributions of the paper lie in the template-based modelling for generating personalised finger bone models and a “3 layer cascade cable-driven system” for the pulley systems, which achieves the full actuation.

The rest of the paper is organised as follows. Section 2 describes the model of our robotic finger. Section 3 presents our method for the design and fabrication of our robotic finger in detail. Section 4 reports the experiments of evaluating the performance of the designed finger using the diagram of motion and Section 5 concludes the paper.

II. MODEL OF THE ROBOTIC FINGER

A. Human hand anatomy

Under the skin, the human hand has a multipart structure which is combined with different human tissues. The most important elements of the structure are bones, joints, ligaments, tendons, muscles, nerves and blood vessels [2] (Figure 2), among which the first five play dominant roles in the dynamics of hand. The joint serves as the linkage of the bones. It has a complex structure containing ligaments and other fine tissues (Figure 3). Each finger has three joints. For the middle finger, starting from fingertips to the palm, there are Metacarpophalangeal (MCP), Proximal Interphalangeal (PIP) and Distal Interphalangeal (DIP) joints. The PIP and DIP joints work as two simple 1-DOF hinge joints for the extension and flexion motion.

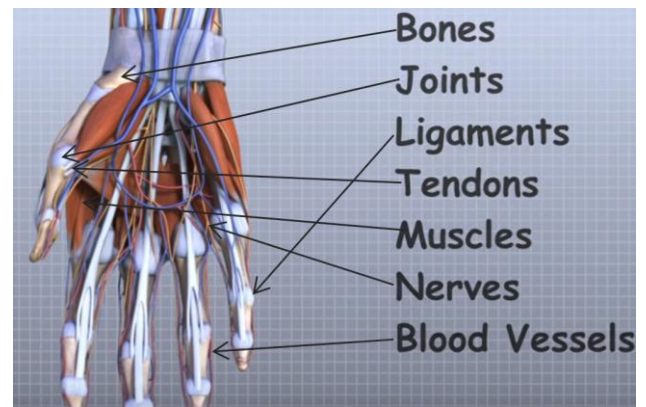


Fig. 2. Human hand anatomy [2].

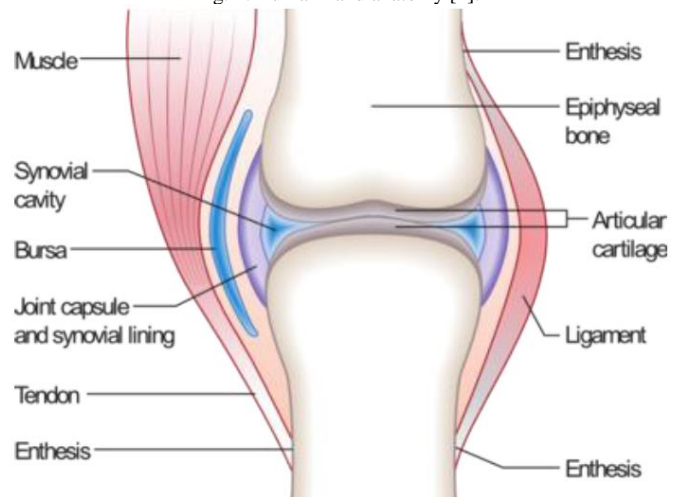


Fig. 3. A typical Joint (Image source: Madhero88/Wikipedia).

The MCP joint is similar to a 2-DOFs saddle joint giving both flexion-extension and abduction-adduction motion. Other joints have insignificant motion (less than 5 degrees) and are neglected in most studies of the hand [8]. The muscles are attached to and actuate bones through the tendons. From the engineering point of view, bones and joints work as a complete mechanical construction. It enables the middle finger to have 4 DOFs. The muscles and the tendons build the actuation systems which give each joint an individual ROM. The nerves are perceptive and deliver the control signals, while the blood vessels supply the energy. For an APH hand or highly biomimetic hand, the basic problem is how to mimic the hand’s mechanical structure as well as the actuation systems.

B. Biomechanics of the middle finger

The muscles shown in Figure 2 are called intrinsic muscles, while the extrinsic muscles are located at the forearm. Various muscles and tendons work together to give the middle finger’s three joint ranges of motion. Table I lists their names, associated joints and the ROM of the joints for the middle finger. The values of ROM are numerical values with five degrees as a step, which are obtained from previous researches on the hand ROM.

TABLE I. JOINTS AND MUSCLES

Joints	ROM (Deg.) [8, 9]	Muscles, tendons [10]
MCP	Extension 0	Extensor Digitorum Communis (EDC)
	Flexion 90	Medial Band (MB)
	Ulnar deviation 25	Dorsal Interossei (DI)
	Radial deviation 15	Palmar Interossei (PI) Lumbrical (LUM)
PIP	Extension 0	Central Slip (CS)
	Flexion 110	Lateral Band (LB) Flexor Digitorum Superficialis (FDS)
DIP	Extension 0	Terminal Extensor (TE)
	Flexion 70	Flexor Digitorum Profundus (FDP)

The top part of Figure 4 shows that the tendons are possibly connected to more than one bone through multiple vinculum. As a result, MCP and PIP are able to move independently. The motion of DIP is affected by PIP, but it is still an independent joint.

From the posterior view of Figure 4, the extensor expansion (hood) covers the bones like a big net. From the lateral view, the FDP and FDS tendons are connected to bones just like cables. They are tightly held in a pulley system and are combined with tendon sheaths (Refer to Figure 4’s bottom part). The tendon sheaths play an important role in regulating the motion of the finger while holding the tendon’s position. It allows the tendon to move horizontally and actuate one or more rotational motion of the finger joints.

C. Finger motion and actuation

The fingers of existing robotic hands have limitations in motion. For example, their DIP and PIP work synchronously as an under-actuation system [11]. As a result, the hand is difficult to bend the DIP alone (Refer to Figure 10 from Pose 1 to Pose 2). According to hand grasp taxonomy, most grasping actions require flex DIP, PIP and MCP joints of the finger to work independently at the same time [12, 13]. Most existing robotic hand design makes use of underactuation systems to control the fingers, which leads to the number of the actuator to be less than the DOF of the fingers. For instance, InMoov hand [14], Xu et al.’s hand [5], and Nadine hand [15-17] just use one actuator to control the flexion of all three joints of one finger. Under the condition of MCP and PIP bending to 90 degrees, we can actually get much better control for the DIP joint (Refer to Figure 10 from Pose 7 to Pose 8).

Note that underactuation design reduces the number of required actuators and the total control complexity. It also greatly reduces the ROM of the finger. In order to mimic all the possible gestures made by human hand, fingers should be fully actuated with the actual DOFs and ROMs. We design a 4 DOFs robotic finger towards this goal.

III. DESIGN AND FABRICATION OF OUR ROBOTIC FINGER

A. Bones

The bones of the human hand have an irregular shape with smooth boundary surfaces, which makes it difficult to model them manually. The human hand has a similar structure but in quite different dimensions.

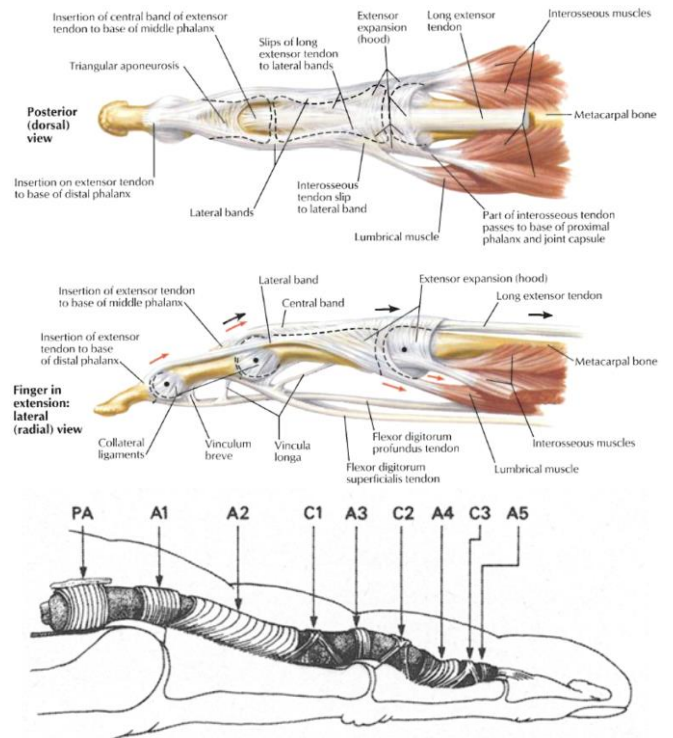


Fig. 4. Top and middle: Finger anatomy without pulley system [18] and Bottom: the pulley systems for flexor tendon [19].

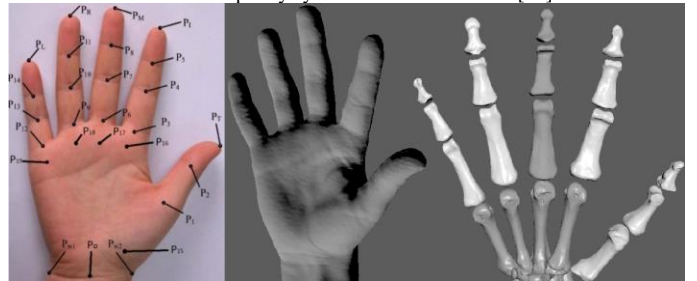


Fig. 5. 3D modelling of the bones of hand from a real hand.

We propose a template-based approach to create customised 3D models of bones for a particular human hand. The approach consists of capturing the real data of the human hand, identifying the landmark points and adapting a template model. Specifically, we have a template of the 3D model for finger bones of a human hand which get from the 3D scan. It is a triangular mesh model and can be converted into STL (sterolithography) format for 3D printing. To create a personalised finger bone model, we use a hand-held 3D scanner (such as “Go!SCAN 20TM”) to scan the real human hand, which yields a 3D mesh model with the help of the corresponding software (Middle of Figure 5). Then we identify the landmarks on the 3D model, as shown in Figure 5 (left). Similar to [17], we calculate the size of the bones according to the 3D coordinate of the hand’s landmarks [20]. Finally, we stretch the template model to fit the calculated sizes and also add holes in each bone for holding the artificial tendon. The implementation of the approach is done by writing script codes in software MAYA™.

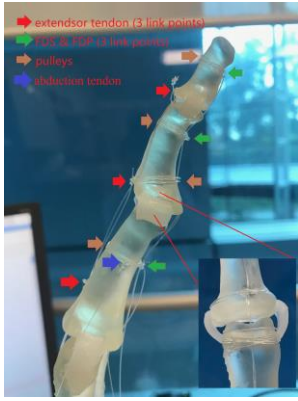


Fig. 6. Tendons and joints of the finger.

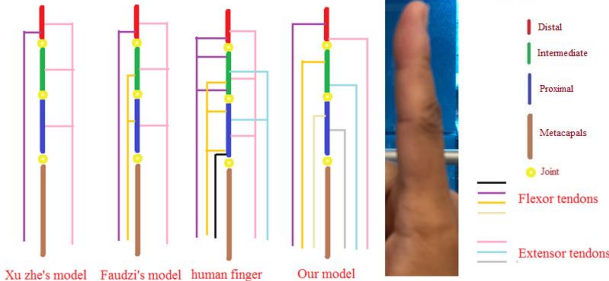


Fig. 7. Comparison of finger actuation systems.

Human finger bones are quite firm with Young's modulus around 10 GPa. We 3D-print the bones using firm material (rs-f2-gpcl-04) with "Form2™" 3D printer. This material's Young's modulus value is 2.8 GPa. As most material is in the range of 10^4 to 10^{12} Pa [7], rs-f2-gpcl-04 is considered to have similar hardness as the bones of the human hand.

B. Joints

It can be seen from Figure 3 that the finger joint is made of bones, ligaments, bursa, synovial cavity, joint capsule and synovial lining. Previous work did a special and complex design to simulate the bones structure using crochet and gimbal [19]. Recently, [6] presented a robotic finger that uses a few pieces of silicon to represent the ligaments of the joints.

It is difficult and not cost-effective to mimic all tissues and tendons of the joint. Our design of joints has three aims: (1) the joint is able to support the human-like ROM when it is driven by an external force; (2) The friction is low and acceptable, and (3) the joint is simple and easy to make. So we use 1-3mm thickness silicon rubber of rectangular shape to link the joints. It can be inserted through the holes on the bones and fixed by instant adhesive. The silicon is elastic, and it gives a support force to the upper bones, thus reducing the contact surface friction, when the finger is moving (see Figure 6).

C. Tendons

A human finger can be modelled as five main tendons with 12 link points to the bones for the flexion/extension move. We simplify it to a "3 layer cascade cable-driven system" that is controlled by six cables (Figure 7). We use 0.3mm diameter, 10 lbs Nylon as our robotic finger's tendon. We twine the cable to the bones to simulate the pulley system (brown arrow in Figure 6).

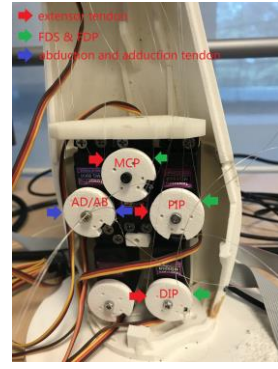


Fig. 8. Motors and servo bed.

To achieve all four DOFs of the middle finger, we use three driven cables to simulate the FDS and FDP tendons for the flexion motion. We tie these three cables to three twined cables (green arrow in Figure 6). We use another set of three cables to simulate the extensor tendon for the extension motion (red arrow in Figure 6). With reference to the position of the real tendon to the bones (Refer to the top and middle of Figure 4), we drill 1mm diameter holes in the 3D model for holding these three cables. We also use two cables to simulate the abduction and adduction motion (blue arrow in Figure 6). All cables go through under the pulley system's twined cables. The other side of the cables is tied to the horn of the motors.

D. Muscles

For human hand, muscles can change their length to pull the tendons and move the fingers. Electric and pneumatic motors are two widely used actuators to simulate muscles for robotic hands. They usually co-work with linkages, camshafts, gears and cables for transmitting the force from the actuator to fingers [21]. Although there are several artificial muscles available that are mentioned in [22], we still choose electric servo motor (Tower Pro™ MG996R) together with driven cables for our actuation solution because of their high accuracy, high torque and low cost [6, 23].

For our robotic finger, we use an open-sourced (InMoov project) forearm with servo bed as the actuation source [24]. In Figure 8, three servos are used to control the flexion and extension of MCP, PIP and DIP joints. Another servo is used for controlling the abduction and adduction (AD/AB) move of the finger.

E. Motion control

Based on Landsmeer's model III [25], the basic equation for modelling the tendon displacement (L) can be simplified to a second-order polynomial approximation [26]:

$$L = (b+h\theta) \theta \quad (1)$$

where b and h are constants determined by the mechanical system, and θ is the corresponding angle rotation.

In this work, we adapt the basic equation for our "3 layer cascade cable driven system":

$$\begin{aligned} L_{\text{pro}} &= (b_1 + h_1 \theta_{\text{pro}}) \theta_{\text{pro}} \\ L_{\text{int}} - L_{\text{pro}} &= (b_2 + h_2 \theta_{\text{int}}) \theta_{\text{int}} \\ L_{\text{dis}} - L_{\text{int}} - L_{\text{pro}} &= (b_3 + h_3 \theta_{\text{dis}}) \theta_{\text{dis}} \end{aligned} \quad (2)$$

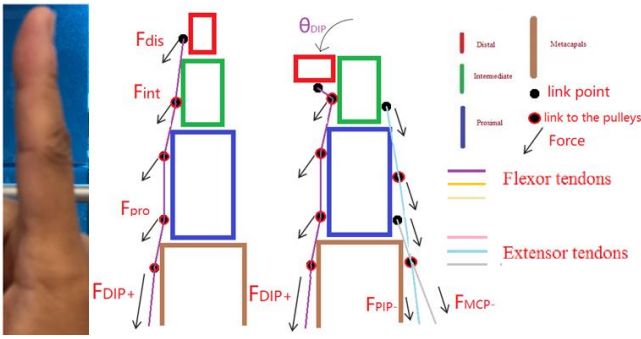


Fig. 9. Dynamic of our robotic finger (bent the DIP).

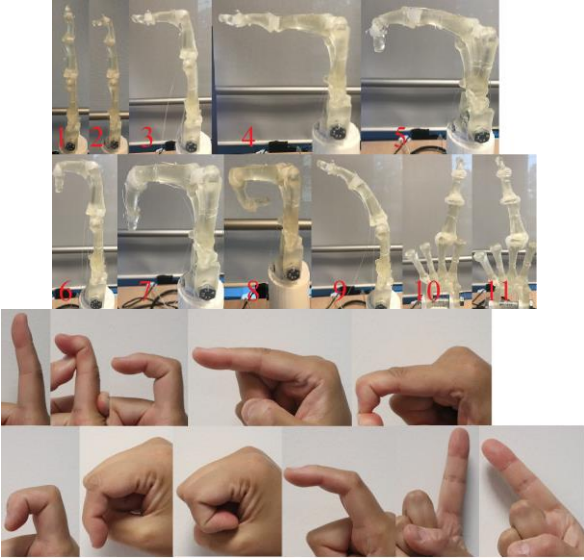


Fig. 10. 11 Pose test results of our robotic finger and real finger

where L_{dis} , L_{int} and L_{pro} are three displacements of three flexor tendons for rotate distal, intermediate and proximal phalanges, respectively.

From Figure 9, the actuator's force F_{dip+} applies to all three phalanges of the finger to create F_{dis} , F_{int} and F_{pro} . F_{dis} rotates the DIP joint and thus changes the pose of the finger. We can use two more forces from the driven cables F_{MCP-} and F_{PIP-} to offset F_{int} and F_{pro} and create the balance for pose 2. This method works in a way similar to the human tendon system in terms of cooperation of actuators and stoppers [2].

IV. PERFORMANCE EVALUATION OF OUR ROBOTIC FINGER

A. Postures

To test the functionality including the extreme motions, we especially use nine finger postures to test the flexion and extension motion, and two more finger postures to test abduction and adduction motion (see Figure 10). Pose 1 is vertical, where all three joints have no flexion. Poses 2~8 are the different combinations of the joints flexion. We introduce pose 9 to mimic the finger in the relax situation. We choose 90 degrees as the standard rotation unit as it is close to the real hand and easy for calculation. Pose 10 shows adduct of the finger and pose 11 shows abduct of the finger.

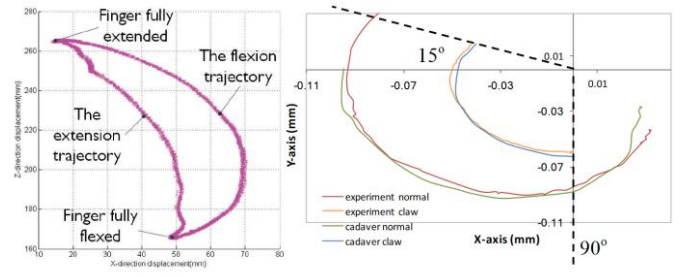


Fig. 11. Dynamic 2D motion range (bottom) and others (top) [5, 6].

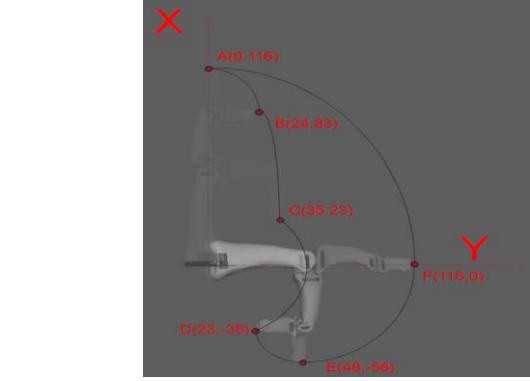


Fig. 12. Our robotic finger works inside the artificial skin

For human hand, when the finger is in extreme poses such as pose 1 and pose 8, we can feel that the tendons are oppositely pulling the fingers to restore to pose 9. From the hand anatomy[2], each finger pose is a balanced result of multiple tendons and vinculum. To reproduce these poses, we use one dimension control (pull/release) of 8 driven cables in different combinations.

B. Motion range

To show the motion range of our robotic system in flexion and extension, we build a 2D coordinate system with the MCP joint as the origin in a virtual environment referenced to [27, 28]. Then we calculate six limit points from the finger pose and then estimate the motion range, as shown in Figure 11. After adding the adduction\abduction motion, the motion range changes in the 3D space, which is similar to the behaviour of a human finger.

We compare our robotic finger to other three representative robotic fingers in terms of DOF, bones design, joints, pulleys, tendons and the actuation ways. The detail is given in Table II.

C. Test with artificial skin

We also test our robotic finger within silicone rubber artificial skin. The result shows that our robotic finger is still able to make clear poses under the artificial skin (Figure 12). The customised artificial hand skin is made of 0 degree (shore A hardness) silicon in 2mm thickness.

TABLE II. COMPARISON

Name	DoF	Bones	Joint	Pulleys	Actuation	Tendons	Comments
Shadow hand's middle finger[4]	3	Manually made 3D model	Rigid structure and screws	Hollowed finger parts	Cable-driven, four joints, 3 two-ways servos	6	Less one DOF than human finger, skeleton structure is unlike human's
Robotic hand's finger by Zhe Xu[5]	2	From cadaver bones (fixed size)	Crocheted volar plate	Laser-cut tendon sheaths	Cable-driven, two one-way servo	2	Highly biomimetic, less 2 DOF than human finger
Robotic Finger by A.A.M Faudzi[6]	2.5	From cadaver bones (fixed size)	Silicon rubber	Tubes	Cable-driven, six one-way muscles	6	3 intrinsic muscles and 3 extrinsic muscles, single EDC
Human finger[2]	4	Real bones	Structured tissues	Tissues	10+ muscles	14	Golden example for our design
Our robotic finger	4	From cadaver bones(Changeable)	Silicon rubber	Nylon cables	Cable-driven, four two-way servos	8	Same DOF and similar ROM as human finger

REFERENCES

- [1] J. K. Salisbury and B. Roth, "Kinematic and force analysis of articulated mechanical hands," *ASME J. Mech., Transm., Autom. Des.*, vol. 105, pp. 35-41, 1983.
- [2] A. M. Agur and A. F. Dalley, "Grant's atlas of anatomy," *Lippincott Williams & Wilkins*, 2009.
- [3] R. Balasubramanian and V. J. Santos, "The human hand as an inspiration for robot hand development," vol. 95: *Springer*, 2014.
- [4] F. Rothling, R. Haschke, J. J. Steil, and H. Ritter, "Platform portable anthropomorphic grasping with the bieiefeld 20-dof shadow and 9-dof tum hand," in *Intelligent Robots and Systems, 2007*, pp. 2951-2956.
- [5] Z. Xu and E. Todorov, "Design of a Highly Biomimetic Anthropomorphic Robotic Hand towards Artificial Limb Regeneration," *2016 Ieee International Conference on Robotics and Automation (Icra)*, pp. 3485-3492, 2016.
- [6] A. A. M. Faudzi, J. Ooga, T. Goto, M. Takeichi, and K. Suzumori, "Index finger of a human-like robotic hand using thin soft muscles," *IEEE Robotics and Automation Letters*, vol. 3, pp. 92-99, 2018.
- [7] D. Rus and M. T. Tolley, "Design, fabrication and control of soft robots," *Nature*, vol. 521, p. 467, 2015.
- [8] R. Degeorges and C. Oberlin, "Measurement of three-joint-finger motions: reality or fancy? A three-dimensional anatomical approach," *Surgical and Radiologic Anatomy*, vol. 25, pp. 105-112, 2003.
- [9] K.-S. Lee and M.-C. Jung, "Ergonomic evaluation of biomechanical hand function," *Safety and health at work*, vol. 6, pp. 9-17, 2015.
- [10] K.-N. An, E. Y. Chao, W. P. Cooney III, and R. L. Linscheid, "Normative model of human hand for biomechanical analysis," *Journal of biomechanics*, vol. 12, pp. 775-788, 1979.
- [11] J. Lin, Y. Wu, and T. S. Huang, "Modeling the constraints of human hand motion," *Workshop on Human Motion, Proceedings*, pp. 121-126, 2000.
- [12] T. Feix, R. Pawlik, H.-B. Schmiemayer, J. Romero, and D. Kragic, "A comprehensive grasp taxonomy," in *Robotics, science and systems: workshop on understanding the human hand for advancing robotic manipulation*, 2009, p. 2.3.
- [13] T. Feix, J. Romero, H.-B. Schmiemayer, A. M. Dollar, and D. Kragic, "The grasp taxonomy of human grasp types," *IEEE Transactions on Human-Machine Systems*, vol. 46, pp. 66-77, 2016.
- [14] G. Langevin, "InMoov-Open Source 3D printed life-size robot," *URL: <http://inmoov.fr>*, License: <http://creativecommons.org/licenses/by-nc/3.0/legalcode>, 2014.
- [15] N. M. Thalmann, L. Tian, and F. Yao, "Nadine: a social robot that can localize objects and grasp them in a human way," in *Frontiers in Electronic Technologies*, ed: Springer, 2017, pp. 1-23.
- [16] L. Tian, N. Magnenat Thalmann, D. Thalmann, and J. Zheng, "The making of a 3D-printed, cable-driven, single-model, lightweight humanoid robotic hand," *Frontiers in Robotics and AI*, vol. 4, p. 65, 2017.
- [17] L. Tian, N. Magnenat-Thalmann, D. Thalmann, and J. Zheng, "A Methodology to Model and Simulate Customized Realistic Anthropomorphic Robotic Hands," in *Proceedings of Computer Graphics International 2018*, 2018, pp. 153-162.
- [18] D. Hu, D. Howard, and L. Ren, "Biomechanical analysis of the human finger extensor mechanism during isometric pressing," *PloS one*, vol. 9, p. e94533, 2014.
- [19] J. R. Doyle, "Anatomy of the finger flexor tendon sheath and pulley system," *Journal of Hand Surgery*, vol. 13, pp. 473-484, 1988.
- [20] Z. Li, C.-C. Chang, P. G. Dempsey, L. Ouyang, and J. Duan, "Validation of a three-dimensional hand scanning and dimension extraction method with dimension data," *Ergonomics*, vol. 51, pp. 1672-1692, 2008.
- [21] J. T. Belter, J. L. Segil, A. M. Dollar, and R. F. Weir, "Mechanical design and performance specifications of anthropomorphic prosthetic hands: A review," *Journal of Rehabilitation Research and Development*, vol. 50, pp. 599-617, 2013.
- [22] M. P. Dicker, A. B. Baker, R. J. Iredale, S. Naficy, I. P. Bond, C. F. Faul, *et al.*, "Light-triggered soft artificial muscles: Molecular-level amplification of actuation control signals," *Scientific reports*, vol. 7, p. 9197, 2017.
- [23] P. Pillay and R. Krishnan, "Application characteristics of permanent magnet synchronous and brushless DC motors for servo drives," *IEEE Transactions on industry applications*, vol. 27, pp. 986-996, 1991.
- [24] G. Langevin, "Hand robot InMoov," 2016.
- [25] J. Landsmeer, "Studies in the anatomy of articulation. I. The equilibrium of the "intercalated" bone," *Acta Morphologica Neerlando-Scandinavica*, vol. 3, p. 287, 1961.
- [26] N. Brook, J. Mizrahi, M. Shoham, and J. Dayan, "A biomechanical model of index finger dynamics," *Medical engineering & physics*, vol. 17, pp. 54-63, 1995.
- [27] N. Magnenat-Thalmann, R. Laperrière, and D. Thalmann, "Joint-dependent local deformations for hand animation and object grasping," In *Proceedings on Graphics interface '88*, 1988, pp. 26 -33.
- [28] N. Magnenat-Thalmann and D. Thalmann, "Handbook of virtual humans," *John Wiley & Sons*, 2005.